Integrated Communication and Control of PV-Based DC Microgrid

Ashraf Khalil[1*]
[1]Electrical and Electronic Engineering Department, Universiti Teknologi Brunei, Brunei
ashraf.sulayman@utb.edu.bn

***Abstract*— The emergence of the renewable energy sources such as the PV, fuel cells and storage systems have shifted the view to DC Microgrid. The inherent PV DC sources provide the compatibility with the DC loads without the need for multiple DC/AC and DC/AC conversions. In the DC Microgrid, the energy sources, storage units and loads are connected to a DC Bus through DC/DC converters. In order to achieve the control tasks and for energy management, the sources should exchange their information through a kind of network. The PV sources controllers communicate through communication network to achieve current sharing. The induced time delay could destabilize the system and it is important to determine the maximum delay margin. The exact delay margin for the stability is computed using the sweeping test and the binary iteration algorithm. The controller achieves good performance even with the fluctuations in the output of the PV sources. The impact of the DC Microgrid parameters and the controller parameters on the delay margin is investigated.**

***Keywords*— DC Microgrid, Delay margin, master/slave, Photovoltaic, stability**

I. Introduction

The Microgrid has emerged as a new technology for the optimum integration of the renewable energy sources into our grid. In the Microgrid the renewable and non-renewable sources are connected in parallel connection to satisfy the load demands. The Microgrid contains distributed energy resources, energy storage systems, and loads. Generally, the Microgrid can be classified into AC Microgrid, DC Microgrid and hybrid Microgrid. DC Microgrid has been recently very active research area because of the inherent nature of the renewable energy sources and the ease of the control comparing with AC Microgrid. The energy management and the control remain the most important aspects in the Microgrid research. The Microgrid can be operated in two modes; grid-connected or islanding. The DC Microgrid can be found in different three topologies; single-bus topology, multi-bus topology and reconfigurable topology (Tomislav Dragievi et al. 2016). A Photovoltaic-based DC Microgrid is shown in Fig. 1.

Recently DC Microgrid has attracted many researchers for the following reasons (Enrique Rodriguez-Diaz et al. 2016): 1) Most of the residential loads are DC, 2) Most of the renewable energy resources generate power in DC form, for example PV arrays, Super-capacitors, batteries and Fuel cells, 3) The reduction in the transmission lines, 4) The electric-vehicles and electric-hybrid vehicles require DC source for charging, 5) It is more efficient than AC distribution systems 6) There is no need to synchronization between the converters which means lower bandwidth communication network can be used, 7) There is no reactive power control, 8) There is no circulating currents or DC offsets. For the aforementioned reasons DC Microgrid and distributed DC system in general, will play main roles in future power system.

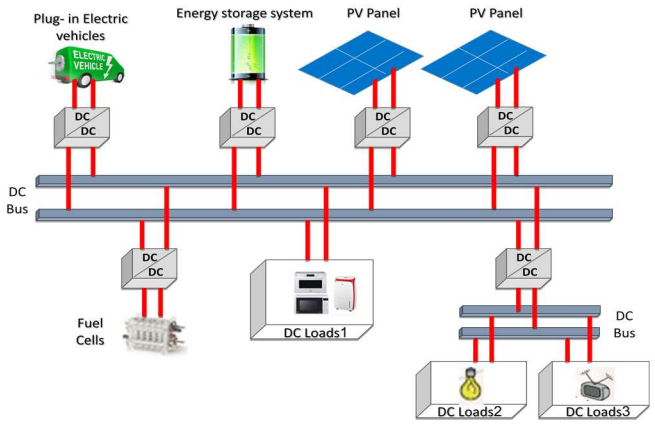

Fig. 1. A Photovoltaic based DC Microgrid

The DC sources can be connected in DC Microgrid without any conversion to AC power, for example, PV panels, fuel cells, super-capacitors, and batteries are inherently DC sources (Amjad Ali et al. 2015). The controller in the DC Microgrid must achieve stable voltage and perfect power sharing. The voltage should remain within a predetermined range even during the transition from the islanding to the grid-connected mode. Many control strategies have been proposed to regulate the voltage of the DC Microgrid. The droop control strategy is one of the most widely adopted control strategy in Microgrid. DC Microgrid is formed by distributed energy units such as PV, wind turbines, fuel cells, etc. in addition to storage units such as batteries and loads. Most of these units are equipped with a power electronic converters which are usually Buck or Boost DC/DC converters or combinations of the two. These generating and storage units operate in parallel to electrify the

loads equally. In order to achieve these tasks, a control strategy is a mandatory. There are three main control strategies that can be implemented in DC Microgrid, which are centralized, decentralized and distributed control strategies.

The DC Microgrid control is a multi-objectives function. Based on Hierarchical control, the control levels can be divided into three levels as shown in Fig. 2 (Lexuan Meng et al. 2017). The energy management and the optimization are carried out in the tertiary control. The power quality and grid synchronization are the responsibility of the secondary control. The primary control performs the voltage, current and power control. The control strategies in DC Microgrid can be classified into active current sharing and droop control. The active sharing can be divided into centralized, master-salve and distributed control strategies (Tomislav Dragicevic et al. 2016). The central controller in the centralized control strategy collects all the required information and sends back the controller commands to the different DC/DC converters in the Microgrid. In the centralized control strategy, all the information is sent to a centralized controller and then the commands are sent back to the system. The main disadvantage of this strategy is the single point of failure and the complexity in the controller design for large and complex interconnected systems. In the distributed and master-slave control strategies there is no central controller but the local controllers communicate with each other through communication network. The communication network induces time delay in the measurements which can lead to system instability. For example in (Khalil et al. 2016), the authors show that if the communication delay is larger than the delay margin, the DC Microgrid becomes unstable. In the droop controller all local information are required by the local controllers and hence there is no delay. The distributed control strategy is very attractive because it requires lower bandwidth communication network and the current sharing accuracy is high (Xiaonan Lu et al. 2016).

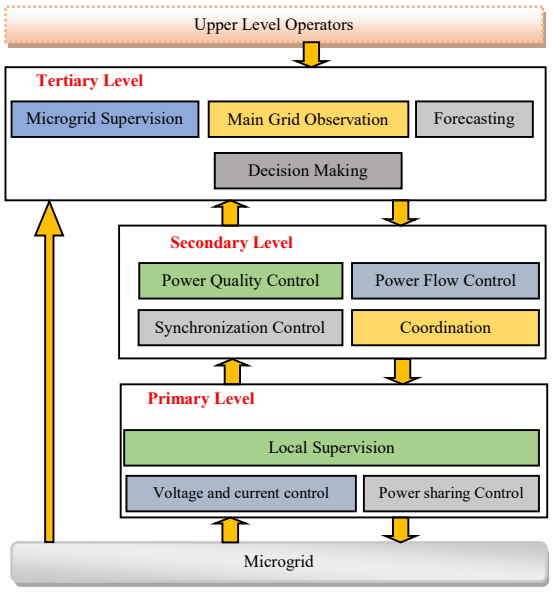

Fig. 2. The control levels in the DC Microgrid (Lexuan Meng et al. 2017)

The classification of the control strategies is shown in Fig. 3. The droop control strategy is a typical decentralized control method. The droop control is flexible and easy to implement, however, the line impedance could affect the power sharing. The droop control is based on linear relation with the voltage. The resistance of the lines results in different voltages in the DC Microgrid. The droop control methods can provide redundancy but the current sharing is not comparable with the master-slave and centralized scheme. Additionally, each parallel converter should not supply a current larger than the maximum current of any converter in the system because in this case one of the converters will supply most of the load. This will result in reducing the lifetime and may lead to overload protection. Many researchers reported the enhancement of the droop control strategy and increasing the accuracy of the current sharing through using communication network (Chunxia Dou et al. 2017;P.P. et al. 2017;Xiaonan Lu, Josep M.Guerrero, & Kai Sun 2016). The deviation of the frequency of the different parallel DC-DC converters will indicate imbalance in the real power and hence a current sharing error. Injecting an ac signal requires phase-locked loop and real power measurement which complicates the controller. In (David J.Perreault et al. 1998;David J.Perreault et al. 1999) a frequency-based current sharing method was proposed. The converters inject ac signal whose frequency depends on the output current. Another approach is to use the DC bus as information carrier which is known as the DC bus signalling (K.Sun et al. 2011;Y.Gu et al. 2014). The master-slave control strategy is a quasi-decentralized control strategy where the information is exchanged between the controllers. The master controller regulates the voltage and generates the reference currents for the slave converters. In the master-slave control strategy, one of the converters is known to be the master while the others are the slaves, the master controller contains the voltage controller while the slaves contain current controllers and have to track the master's reference current (Ashraf Khalil et al. 2015). If the master fails one of the slaves will take his role. In this control strategy there is a transfer of information between the master controller and the slaves' controllers. The master-slave control of a DC Microgrid is investigated in (Li Guo et al. 2014). The analysis is carried out in the z-plane with the discrete-time model of the DC Microgrid and it has been found that the time delay has a strong impact on the stability of the Microgrid. In (Khalil, Elkawafi, Elgaiyar, & Wang 2016), the stability of the DC Microgrid with time varying delay is investigated and the maximum delay margin is calculated using Lyapunov-Krasovskii function approach.

Two centralized control strategies are introduced in (C.Q.Lee et al. 1991), the programmable current distribution control (PCDC) and the maximum current limit control (MCLC). In the MCLC the converters are not always switched on and the number of the active converters is determined by the load condition. The MCLC has higher efficiency because at light loads some of the converters will be switched off.

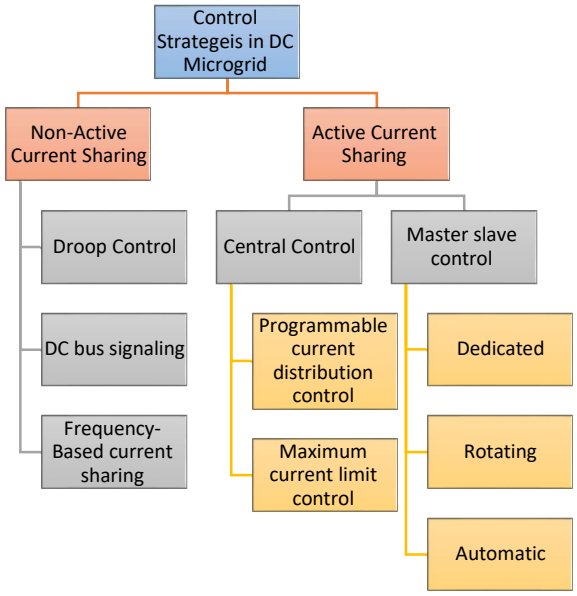

Fig. 3. The control strategies in the DC Microgrid

In (Chaoyu Dong et al. 2017a) the distributed control is suggested for the DC Microgrid control. As the time delay is inherited in the distributed control, the DC Microgrid is modelled as neutral type time delay system. Then a linear matrix inequalities (LMIs) criterion is used to determine the delay margin where the free-weighting matrices are used to decrease the conservativeness of the results. A distributed cooperative optimal control is presented in (Lei Ding et al. 2018). The communication delay is considered and the delay margin is computed for the system where various communications technologies were considered. These are the PLC, fibre-optical, WiMAX, 4G and Microwave. The delay dependent stability of DC Microgrid with hybrid energy storage is investigated in (Chaoyu Dong et al. 2017b). A hierarchical control is proposed to achieve load sharing and a frequency domain method is used to calculate the maximum delay margin. A low communication network is used in (Xiaonan Lu et al. 2014) to enhance the current sharing of the droop control strategy. A novel communication method is presented in (Zhengyu Lin et al. 2018). The DC bus is used as the communication medium where the switching frequency is used as the information. The method has been implemented to three DC/DC converters DC Microgrid. The stabilization of the DC Microgrid is studied in (Yuwen Nie et al. 2017). The distributed control is used to regulate the voltage and achieve current sharing.

The recent advances in wireless networks technology and increased number of distributed DC power systems have resulted in promoting wireless networks as communication medium for the control system. This reduces the complexity and the cost while increasing the reliability. This configuration could provide redundancy and plug-and-play functionality if rotary master-slave is used. When the reference current signals are distributed through wireless network the parallel DC converters system becomes a kind of wireless networked control system (WNCS). The wireless network in the feedback loop offers many advantages for the system such as modularity, simplified wiring, low cost, reduced weight, decentralization of control, integrated diagnosis, simple installation, quick and easy for maintenance, flexible expandability and reconfigurability (Khalil and Wang 2010). The main issues in wireless networks are the time delay and the data loss which can lead to the system performance degradation or losing the stability. The emergence of the wireless networks revolutionized the control industry. Many researchers proposed the wireless network as an alternative to the traditional control networks such as Profibus and Control Area Network in many control applications. In order to achieve stabilization of the system, it is important to compute the maximum delay margin.

In this paper, we investigate the impact of the communication delay on the stability of PV-based DC Microgrid. In the next sections the modelling and the master-slave control of PV-Based Microgrid are described, then a stability criterion in s-domain is used to investigate the stability of the DC Microgrid with the time delay and the fluctuating DC sources caused by the variable solar radiation. Finally, the impact of the DC Microgrid parameters and the controller parameters on the delay margin is investigated.

II. Modelling of PV-based DC Microgrid with Master-Slave Control Strategy

A. The Master-Slave Control Strategy

The DC Microgrid implements master-slave control strategy as shown in Fig. 4. The master controller regulates the voltage and generates the reference current for the master and the slaves. The slave current controller has to track the reference current received from the master controller. The reference current is sent to the slaves through communication network where the time delay is induced.

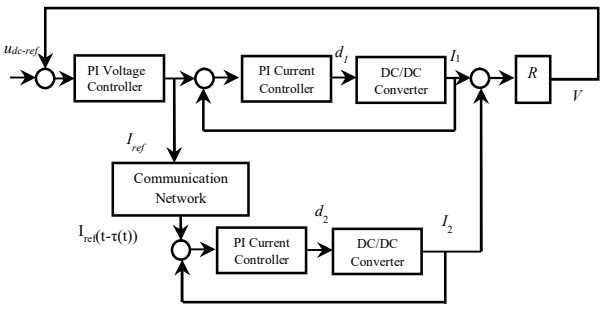

Fig. 4. The DC Microgrid with Master-slave control strategy

The PV arrays are connected to the DC bus through two DC/DC converters as shown in Fig 5 (Mohammad B.Shadmand et al. 2014;Yuan-Chih Chang et al. 2013). The first DC/DC converter extracts the maximum power from the PV array. The second DC/DC converter regulates the voltage and achieves the power sharing. This two stage DC conversion is more efficient than the most efficient DC/AC inverter (Mohammad B.Shadmand, Robert S.Balog, & Haitham Abu-Rub 2014).

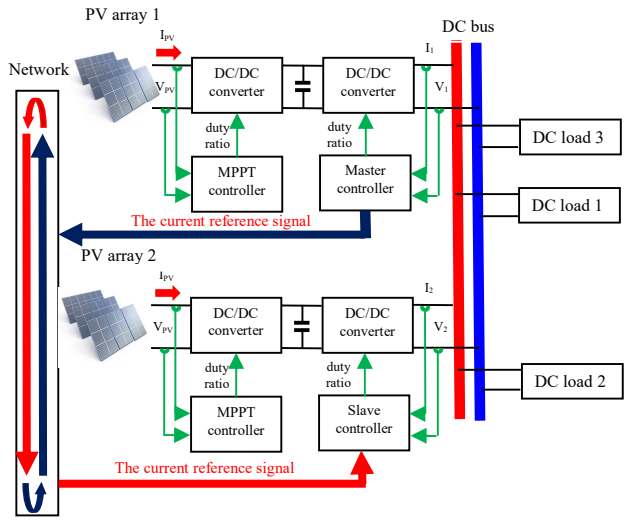

Fig. 5. A PV based DC Microgrid with droop control

B. *The Mathematical Model of the PV Array*

The temporal behaviour of the power variation in a photovoltaic generator is characterized by a standard deviation (dV_{PV}), PV system time response is τ_{PV} and the nominal voltage of the PV array is $V_{PV\text{-}nom}$. The mathematical model used for the PV source is given by (Ashraf Khalil et al. 2017;Elkawafi et al. 2016):

$$V_{PV} = V_{PV\_nom} + \eta \frac{1}{\tau_{PV} s + 1} \sqrt{dV_{PV}} \tag{1}$$

C. *The Mathematical model of the DC Microgrid*

A DC Microgrid contains two DC/DC Boost converters is shown in Fig 6. The Boost converter is a step-up converter where the output voltage can be regulated to be larger than the input voltage. The two converters are connected to the loads through cables which are represented in the figure as series resistance with inductance (R_e and L_e).

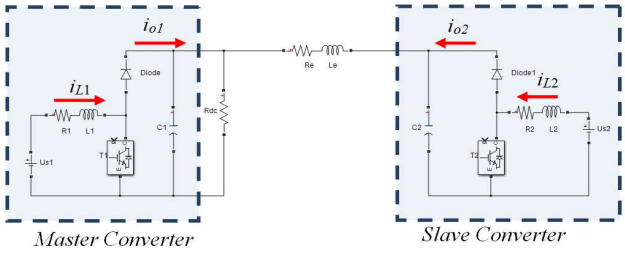

Fig. 6. A DC Microgrid circuit model

The state-space linearized model of two DC/DC Boost converters is given by (Khalil, Elkawafi, Elgaiyar, & Wang 2016;Li Guo, Yibin Feng, Xialin Li, Chengshan Wang, & Yunwei Li 2014):

$$\dot{x}_p(t) = A_p x_p(t) + B_p u_p(t) \tag{2}$$

where;

$$\dot{x}_p(t) = \begin{bmatrix} \Delta u_{c1} & \Delta i_{L1} & \Delta u_{c2} & \Delta i_{L2} & \Delta i_o \end{bmatrix}^T,\ u_p(t) = \begin{bmatrix} d_1 & d_2 \end{bmatrix}^T$$

A_p and B_p are the state and the input matrix respectively, d_1 and d_2 are the duty ratio signals of the master and the slave respectively which are used as control input in this model, Δu_{c1} and Δu_{c2} are the output voltages of the master and the slave respectively, Δi_{L1} and Δi_{L2} are the inductor currents of the first and the second converter respectively, and Δi_o is the output current, A_p and B_p are defined as:

$$A_p = \begin{bmatrix} -\frac{1}{R_{dc}C_1} & \frac{1-D_1}{C_1} & 0 & 0 & \frac{1}{C_1} \\ -\frac{1-D_1}{L_1} & -\frac{R_1}{L_1} & 0 & 0 & 0 \\ 0 & 0 & 0 & \frac{1-D_2}{C_2} & -\frac{1}{C_2} \\ 0 & 0 & -\frac{1-D_2}{L_2} & -\frac{R_2}{L_2} & 0 \\ -\frac{1}{L_e} & 0 & \frac{1}{L_e} & 0 & \frac{R_e}{L_e} \end{bmatrix} \tag{3}$$

$$B_p = \begin{bmatrix} -\frac{I_{L1}}{C_1} & 0 \\ \frac{U_{c1}}{L_1} & 0 \\ 0 & -\frac{I_{L2}}{C_2} \\ 0 & \frac{U_{c2}}{L_2} \\ 0 & 0 \end{bmatrix} \tag{4}$$

The parameters in A_p and B_p are shown in Fig. 6. It should be noted that D_1, D_2, U_{c1}, U_{c2}, I_{L1} and I_{L2} are the DC operating points of the DC Microgrid. The detailed structure of the master and the slave controllers are shown in Fig. 7.

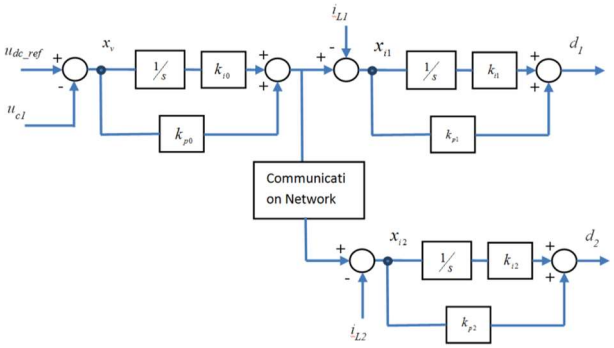

Fig. 7. The master and the slave controllers

The state-space model of the master and the slave controllers are given by:

$$\begin{bmatrix} \dot{x}_v \\ \dot{x}_{i1} \\ \dot{x}_{i2} \end{bmatrix} = \begin{bmatrix} -1 & 0 & 0 & 0 & 0 \\ -k_{p0} & -1 & 0 & 0 & 0 \\ 0 & 0 & 0 & -1 & 0 \end{bmatrix} \begin{bmatrix} \Delta u_{c1} \\ \Delta i_{L1} \\ \Delta u_{c2} \\ \Delta i_{L2} \\ \Delta i_o \end{bmatrix} + \begin{bmatrix} 0 & 0 & 0 \\ k_{i0} & 0 & 0 \\ 0 & 0 & 0 \end{bmatrix} \begin{bmatrix} x_v \\ x_{i1} \\ x_{i2} \end{bmatrix}$$

$$+ \begin{bmatrix} 0 & 0 & 0 & 0 & 0 \\ 0 & 0 & 0 & 0 & 0 \\ -k_{p0} & 0 & 0 & 0 & 0 \end{bmatrix} \begin{bmatrix} \Delta u_{c1}(t-\tau) \\ \Delta i_{L1}(t-\tau) \\ \Delta u_{c2}(t-\tau) \\ \Delta i_{L2}(t-\tau) \\ \Delta i_o(t-\tau) \end{bmatrix} + \begin{bmatrix} 0 & 0 & 0 \\ 0 & 0 & 0 \\ k_{i0} & 0 & 0 \end{bmatrix} \begin{bmatrix} x_v(t-\tau) \\ x_{i1}(t-\tau) \\ x_{i2}(t-\tau) \end{bmatrix} \tag{5}$$

$$\begin{bmatrix} d_1 \\ d_2 \end{bmatrix} = \begin{bmatrix} -k_{p1}k_{p0} & -k_{p1} & 0 & 0 & 0 \\ 0 & 0 & 0 & -k_{p2} & 0 \end{bmatrix} \begin{bmatrix} \Delta u_{c1} \\ \Delta i_{L1} \\ \Delta u_{c2} \\ \Delta i_{L2} \\ \Delta i_o \end{bmatrix} + \begin{bmatrix} k_{p1}k_{i0} & k_{i1} & 0 \\ 0 & 0 & k_{i2} \end{bmatrix} \begin{bmatrix} x_v \\ x_{i1} \\ x_{i2} \end{bmatrix} + \begin{bmatrix} 0 & 0 & 0 \\ k_{p2}k_{i0} & 0 & 0 \end{bmatrix} \begin{bmatrix} x_v(t-\tau) \\ x_{i1}(t-\tau) \\ x_{i2}(t-\tau) \end{bmatrix} + \begin{bmatrix} 0 & 0 & 0 & 0 & 0 \\ -k_{p2}k_{p0} & 0 & 0 & 0 & 0 \end{bmatrix} \begin{bmatrix} \Delta u_{c1}(t-\tau) \\ \Delta i_{L1}(t-\tau) \\ \Delta u_{c2}(t-\tau) \\ \Delta i_{L2}(t-\tau) \\ \Delta i_o(t-\tau) \end{bmatrix} \quad (6)$$

where k_{p0} and k_{i0} are the PI controller gains of the master voltage controller, k_{p1} and k_{i1} are the PI controller gains of the master current controller, and k_{p2} and k_{i2} are the PI controller gains of the slave current controller. Equations (5) and (6) can be written in matrix form as:

$$\dot{x}_c(t) = Ex_p(t) + Fx_c(t) + E_d x_p(t-\tau(t)) + F_d x_c(t-\tau(t)) \quad (7)$$

$$u_p(t) = Cx_p(t) + Dx_c(t) + C_d x_p(t-\tau(t)) + D_d x_c(t-\tau(t)) \quad (8)$$

Substituting (8) into (2) and writing the resulting equation in matrix form along with (7) we get;

$$\begin{bmatrix} \dot{x}_p(t) \\ \dot{x}_c(t) \end{bmatrix} = \begin{bmatrix} A_p + B_pC & B_pD \\ E & F \end{bmatrix} \begin{bmatrix} x_p(t) \\ x_c(t) \end{bmatrix} + \begin{bmatrix} B_pC_d & B_pD_d \\ E_d & F_d \end{bmatrix} \begin{bmatrix} x_p(t-\tau(t)) \\ x_c(t-\tau(t)) \end{bmatrix} \quad (9)$$

Equation (9) can be further written as:

$$\dot{x}(t) = Ax(t) + A_d(t-\tau(t)) \quad (10)$$

where;

$$A = \begin{bmatrix} A_p + B_pC & B_pD \\ E & F \end{bmatrix} \quad A_d = \begin{bmatrix} B_pC_d & B_pD_d \\ E_d & F_d \end{bmatrix} \quad x(t) = \begin{bmatrix} x_p(t) \\ x_c(t) \end{bmatrix}$$

To find the maximum delay margin, τ_d, we transform (10) using Laplace transform and then the characteristics equation becomes:

$$sI - A - A_d e^{-s\tau} = 0 \quad (11)$$

Equation (11) is a transcendental equation and have been the subject of the research for many years. The system is asymptotically stable for a given delay if all the roots of (11) lie on the left half plane. The free delay system is assumed to be stable and all the roots are on the left half plane. For some value of the delay one or more roots will cross the imaginary excess. One of the approaches is to replace s with $j\omega$ and perform the analysis in the frequency domain.

III. Delay Margin Computation Using Sweeping Test

Time delay systems can be either delay-independent or delay dependent. The delay-dependent system is asymptotically stable for $\tau < \tau_d$, marginally stable for $\tau = \tau_d$, and unstable for $\tau > \tau_d$. The delay independent system is asymptotically stable for any positive value of the time delay.

For the DC Microgrid system represented by (10) to be asymptotically stable independent of delay, we must have:

$$\det(sI - A - A_d e^{-s\tau}) \neq 0 \qquad \forall s \in C_+ ,\ \forall \tau \geq 0 \quad (12)$$

where C_+ is the open right half plane. If (12) is satisfied, then there are no positive roots for any value of the time delay. The delay dependent stability implies that for time delays less than the delay margin the system is asymptotically stable and all the roots are on the closed left half plane, and when the time delay exceeds the delay margin the system becomes unstable and some roots will be on the right half plane. In this manner, the roots will cross the imaginary axis when $\tau = \tau_d$. To simplify the analysis we replace s by $j\omega$. Now, we turn our attention to find the delay that produce frequencies on the imaginary axis. Then system (10) is said to be asymptotically stable independent of delay if (Jie Chen 1995):

$$\det(j\omega I - A - A_d e^{-j\omega\tau}) \neq 0 \qquad \forall \omega \in (0,\infty) ,\ \tau \geq 0 \quad (13)$$

If (13) is not satisfied for some values of ω then the system is delay-dependent stable. Now the problem is to find the crossing frequency, ω_c , where the roots cross the imaginary axis. To find the crossing frequencies we use the spectral radius in the following definition.

Definition 1 (Keqin Gu et al. 2003):

The spectral radius of two matrices pair is defined as:

$$\underline{\rho}(A, A_d) := \min\left\{|\lambda| \,\middle|\, \det(A - \lambda A_d) = 0\right\} \quad (14)$$

where $\lambda_i(A)$ is the i^{th} eigenvalue of the matrix A and $\lambda_i(A, A_d)$ is the generalized eigenvalue of matrix pair A, and A_d.

The computation of the delay margin is carried out in the ω domain. To compute the maximum delay margin we adopt the sweeping test (Jie Chen and Haniph A.Latchman 1995). The sweeping test is very valuable tool especially with the advances in the computing capabilities of the today's computers. The seeping test is better for its simplicity with less computation and accurate results. To find the delay margin of the system we use the following theorem.

Theorem 1:(Keqin Gu, Vladimir L.Kharitonov, & Jie Chen 2003)

For the system (10) stable at τ_d=0, i.e., A+A_d is stable and $rank(A_d)$=q, we define

$$\bar{\tau}_i := \begin{cases} \min\limits_{1\leq k\leq n} \dfrac{\theta_k^i}{\omega_k^i}, & if \quad \lambda_i(j\omega_k^i I - A, A_d) = e^{-j\theta_k^i} \\ & for \quad some \quad \omega_k^i \in (0,\infty), \theta_k^i \in [0, 2\pi] \\ \infty, & \underline{\rho}(j\omega I - A, A_d) > 1 \quad \forall \omega \in (0,\infty) \end{cases}$$

Then $\tau_d := \min_{1\leq i\leq q} \bar{\tau}_i$, and the system in (10) is stable for all $\tau \in [0, \tau_d)$ and becomes unstable at $\tau = \tau_d$.

Proof (Jie Chen et al. 1994;Jie Chen 1995;Jie Chen & Haniph A.Latchman 1995;Keqin Gu, Vladimir L.Kharitonov, & Jie Chen 2003):

The system (10) is stable independent of the time delay if the following condition is satisfied:

$$\underline{\rho}(j\omega I - A, A_d) = \underline{\rho}(j\omega I - A, A_d e^{-j\omega\tau}) > 1 \text{ for } \omega > 0,\ \tau \geq 0 \quad (15)$$

Condition (15) implies that the system is stable with $\tau = 0$, that is, $\det(A + A_d) \neq 0$. Now we assume that the system becomes unstable for some value of τ. This means $\tau_d < \infty$. Now, we assume that:

$$\det(j\omega I - A - A_d e^{-j\omega\tau}) \neq 0 \quad \forall \omega \in (0, \infty) \quad (16)$$

This can be true for $\omega \neq \omega_k^i$, and consequently at this condition:

$$\left|\lambda_i(j\omega I - A, A_d)\right| \neq 1 \quad i = 1, ..., n \quad (17)$$

For any $\tau \in [0, \tau_d)$, $\tau\omega_k^i \neq \theta_k^i$ we must have:

$$\det(j\omega_k^i I - A - A_d e^{-j\omega_k^i \tau}) \neq 0 \quad (18)$$

When $\tau = \tau_d$ there is a pair (ω_k^i, θ_k^i) that satisfy $\tau_d = \theta_k^i / \omega_k^i$, and consequently:

$$\det(j\omega_k^i I - A - A_d e^{-j\omega_k^i \tau_d}) = \det(j\omega_k^i I - A - A_d e^{-j\theta_k^i}) = 0 \quad (19)\ \square$$

Corollary 1 (Kequin Gu et al. 2003): The system (10) is stable independent of delay if and only if:

(i) A is stable,

(ii) $A+A_d$ is stable, and

(iii) $\underline{\rho}(j\omega I - A, A_d) > 1, \quad \forall \omega > 0$

The three conditions in Corollary 1 represent the delay independent stability, where (i) states that the system is stable at $\tau = 0$, (ii) the system is stable at $\tau = \infty$ and (iii) the system is stable for every τ in the range $\tau \in [0, \infty)$.

Theorem 1 determines both the delay independent and the delay dependent stability. First we can verify the delay independent stability by checking the following condition:

$$\underline{\rho}(j\omega I - A, A_d) > 1 \quad \forall \omega \in (0, \infty)$$

If the above condition is satisfied then the system is stable independent of time delay and if it is not satisfied for some values of ω that makes $\underline{\rho}(j\omega I - A, A_d) < 1$ then we calculate the crossing frequencies using the following algorithm:

Step 1: With the given system parameters, compute A and A_d. Using the sweeping test, check if the system is stable independent of delay or not, that is $\underline{\rho}(j\omega I - A, A_d) > 1$ for $\omega \in (0, \infty)$. If for some values of ω, $\underline{\rho}(j\omega I - A, A_d) = 1$, then proceed to step 2, otherwise the system is stable independent of the time delay.

Step 2: Define a range $\omega \in [\omega_1, \omega_2]$. At ω_1 the spectral radius $\underline{\rho}(j\omega I - A, A_d) < 1$ and at ω_2 the spectral radius $\underline{\rho}(j\omega I - A, A_d) > 1$. Now the crossing frequency, ω_c, lies in the range from ω_1 to ω_2, in other words $\omega_c \in [\omega_1, \omega_2]$.

Step 3: Use the binary iteration to find the crossing frequency, ω_c, with a given error tolerance ω_e (Elkawafi, Khalil, Elgaiyar, & Wang 2016;Khalil, Elkawafi, Elgaiyar, & Wang 2016). We set $\omega_{new} = (\omega_1 + \omega_2)/2$, if $\underline{\rho}(j\omega_{new} I - A, A_d) > 1$ then $\omega_2 = \omega_{new}$ and if $\underline{\rho}(j\omega_{new} I - A, A_d) < 1$ then $\omega_1 = \omega_{new}$. Now the search range is reduced every iteration until the desired accuracy is reached.

Step 4: When the desired accuracy is reached we calculate θ_k^i, the crossing angles, through solving $\lambda_i(j\omega_k^i I - A, A_d) = e^{-j\theta_k^i}$. Finally, $\tau_d = \min_{1 \leq k \leq n} \theta_k^i / \omega_k^i$ is the desired delay margin.

IV. Case Study

A case study DC Microgrid consists of two Boost converters is chosen, the parameters are given in Table I.

TABLE I DC Microgrid Parameters

Parameter	Value	Parameter	Value	Parameter	Value
C_1	4000 μF	R_1	0.04 Ω	f_s	10 kHz
C_2	2000 μF	R_2	0.04 Ω	U_{s1}	550 V
L_1	5 mH	k_{p0}	1	U_{s2}	550 V
L_2	5 mH	k_{i0}	100	U_{c1}	750 V
R_e	0.037 Ω	k_{p1}	0.01	U_{c2}	750 V
L_e	0.1 mH	k_{i1}	10	V_{ref}	750 V
R_{dc}	40 Ω	k_{p2}	0.02	D_1	0.27
I_{L1}	13 A	k_{i2}	40	D_2	0.27
I_{L2}	13 A				

A. Delay Margin Computation

Using the parameters in Table I, the DC Microgrid is implemented in Matlab/Simulink. The output voltage without time delay is shown in Fig. 8. The output voltage is stable at 750 V even with the fluctuations in the DC PV sources. The DC voltages of the two sources (u_{s1} and u_{s2}) are shown in Fig .9. The output PV voltages of the two arrays change from 460 V to 540 V, however the DC bus voltage remains constant at 750 V which shows the effectiveness of the control strategy.

The currents passing through the inductors are shown in Fig. 10. It is clear that the current sharing is achieved. Solving (19) the delay margin (maximum allowable delay bound) (Khalil and Wang 2011), the crossing frequency is 146.1951 *Hz* and the crossing angle is 1.9588 *rad* which makes the delay margin 13.3985 *ms*. The spectral radius, ρ, as function of the frequency is shown in Fig. 11. When the frequency is larger than 146.1951 Hz, the spectral radius becomes larger than 1. The output voltage with different time delays is shown in Fig 12. The system is nearly stable with 13.3985 *ms* and unstable with 14 *ms* which proves the accuracy of the results.

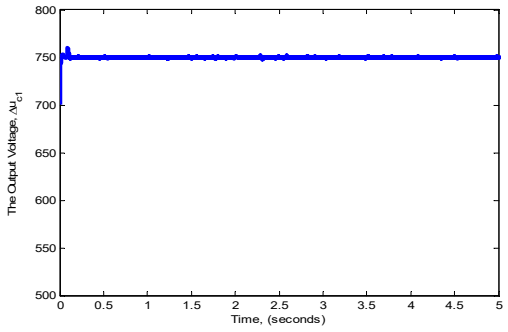

Fig. 8. The output voltage without time delay

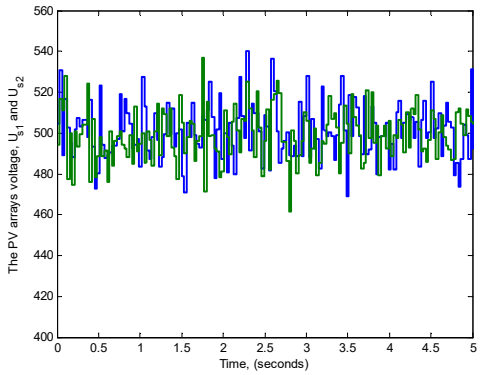

Fig. 9. The two PV sources voltages, u_{s1} and u_{s2}

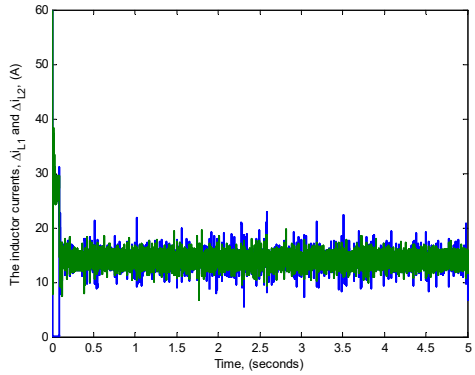

Fig. 10. The inductor currents, Δi_{L1} and Δi_{L2}

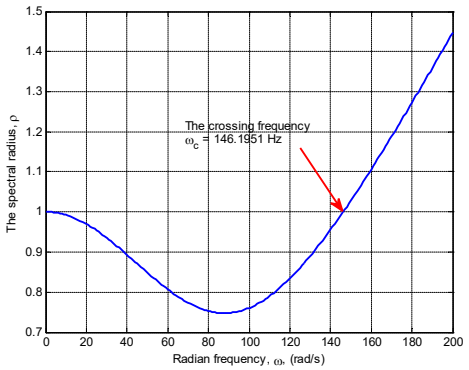

Fig. 11. The spectral radius as function of the frequency

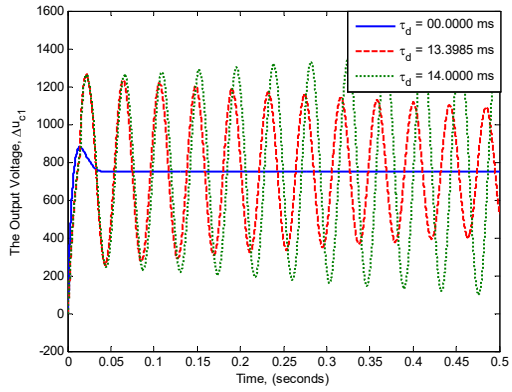

Fig. 12. The output voltage with different time delays

B. *Delay Margin Computation*

The load is very important parameter in the stability of the DC Microgrid (Li Guo, Yibin Feng, Xialin Li, Chengshan Wang, & Yunwei Li 2014). The delay margin as a function of the load resistance is shown in Fig 13. The delay margin decreases with increasing the load resistance. The delay margin as function of the capacitors C_1 and C_2 is shown in Fig. 14. As can be seen from Fig. 14, the delay margin decreases with increasing the capacitances in the range (0-1 mF). When the capacitance increases beyond 1 mF, the delay margin increases with increasing the capacitance. The DC sources of the two DC/DC converters are supplied through two PV arrays where their voltages are subject to variations because of the variable radiation and temperature. The delay margin as function of the input DC sources is shown in Fig. 15. The delay margin decreases linearly with increasing the input DC sources. It is found that the other parameters have a small effect on the delay margin. For example, the delay margin as function of the variations in R_{L1} and R_{L2} is shown in Fig. 16.

The impact of the controllers' parameters on the delay margin is also investigated. The delay margin as function of the master voltage controller parameters is shown in Fig. 17 and 18. The delay margin decreases with increasing k_{i0} and increases with increasing k_{p0}. The delay margin as function of the master current controller and the slave current controller is shown in Figs. 19-22.

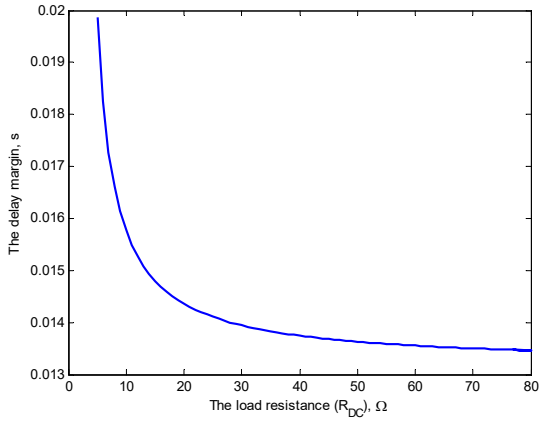

Fig. 13. The delay margin as function of the load

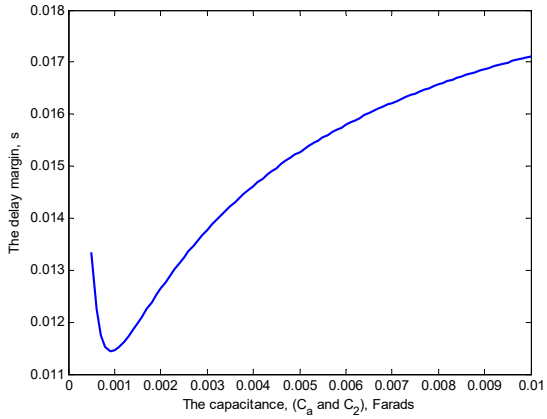

Fig. 14. The delay margin as function of the capacitances

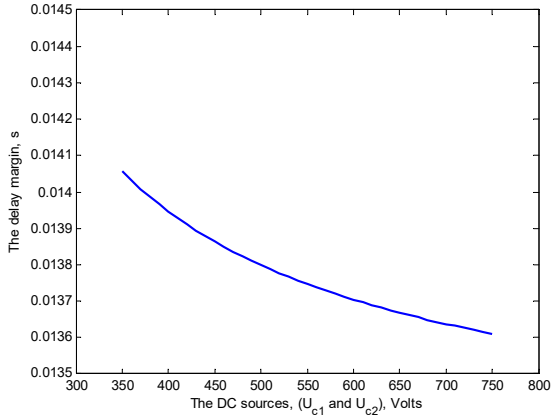

Fig. 15. The delay margin as function of the DC sources

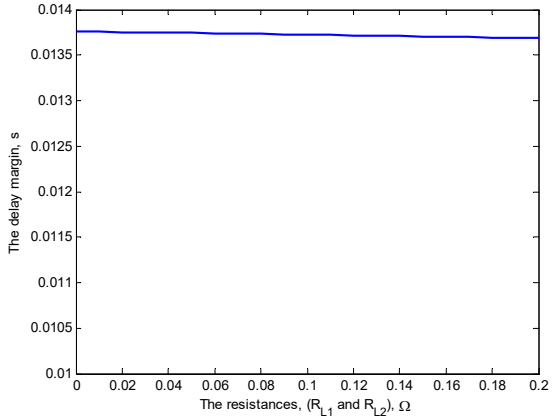

Fig. 16. The delay margin as function of R_{L1} and R_{L2}

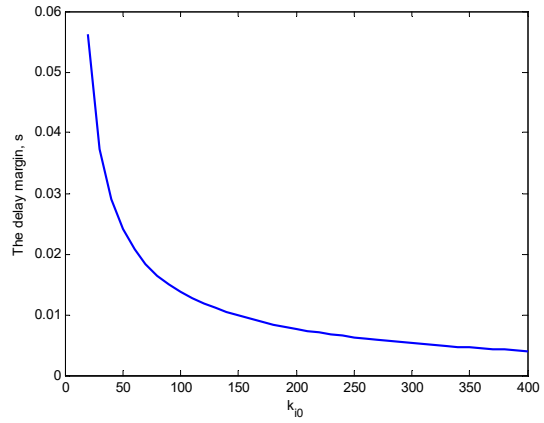

Fig. 17. The delay margin as function of k_{i0}

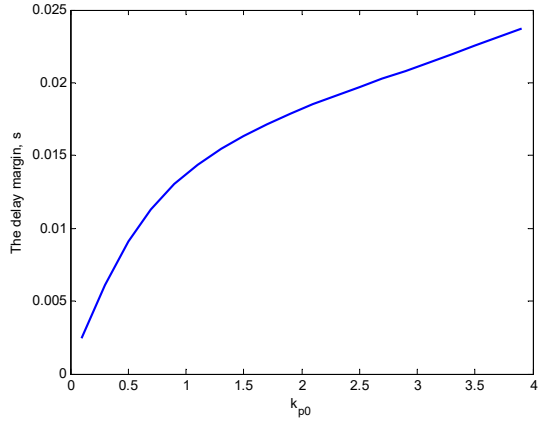

Fig. 18. The delay margin as function of k_{p0}

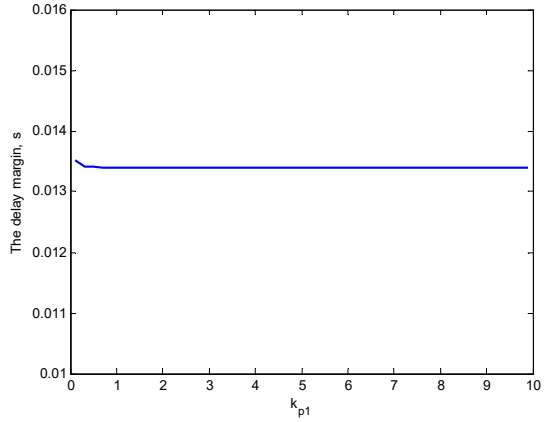

Fig. 19. The delay margin as function of k_{p1}

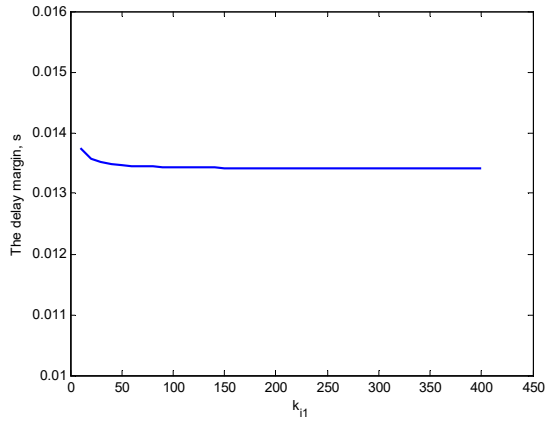

Fig. 20. The delay margin as function of k_{i1}

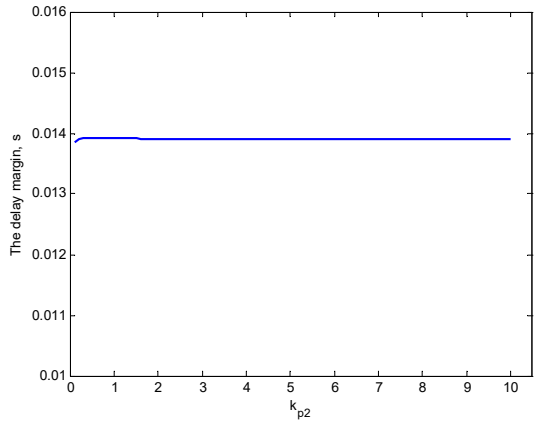

Fig. 21. The delay margin as function of k_{p2}

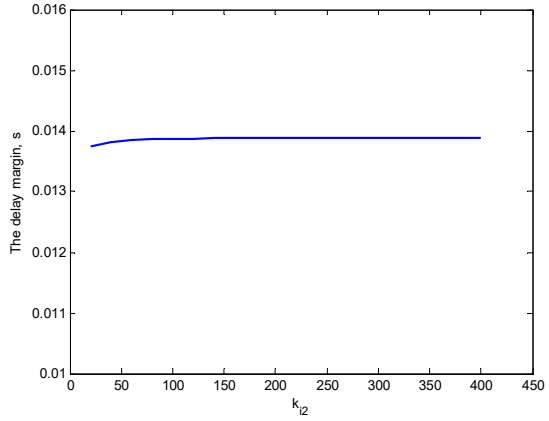

Fig. 22. The delay margin as function of k_{i2}

V. CONCLUSIONS

This paper presents the delay dependant stability analysis of PV based DC Microgrid. The DC Microgrid implements a Master-Slave control strategy where the reference current signal is distributed through communication network. The DC Microgrid forms a time delay system. The delay margin that determines the stability of the system is calculated using the sweeping test and the binary iteration algorithm. The impact of the system and the controller parameters on the delay margin is investigated. The load resistance and the capacitor values have strong effect on the delay margin. It is found that the delay margin decreases with increasing the load resistance while it increases with increasing the capacitor values. The delay margin depends on the master voltage controller, while the parameters of the master current controller and the slave current controller do not affect the delay margin. The delay margin decreases with increasing the integral gain and increases with increasing the proportional gain of the master voltage controller.

REFERENCES

[1] Amjad Ali, Ajmal Farooq, Zeeshan Muhammad, Furqan Habib, & Sheraz Alam Malik 2015. A Review: DC Microgrid Control and Energy Management System. International Journal of Electrical and Electronic Science, 2, (2) 24-30

[2] Ashraf Khalil, Omar Mohamed, & Jihong Wang Networked control of parallel DC/DC buck converters, In 2015 IEEE Jordan Conference on Applied Electrical Engineering and Computing Technologies (AEECT), Amman: pp. 1-6.

[3] Ashraf Khalil, Zakariya Rajab, Asma Alfergani, & Omar Mohamed 2017. The impact of the time delay on the load frequency control system in microgrid with plug-in-electric vehicles. Sustainable Cities and Society, 35, (2017) 365-377

[4] C.Q.Lee, K.Siri, & T.-F.Wu Dynamic current distribution controls of a parallel connected converter system ,In Power Electronics Specialists Conference, 1991. PESC '91 Record., 22nd Annual IEEE, Cambridge, MA: pp. 875-881.

[5] Chaoyu Dong, Fanghong Guo, Hongjie Jia, Yan Xu, Xiaomeng Li, & eng Wang 2017a. DC Microgrid Stability Analysis Considering Time Delay in the Distributed Control. Energy Procedia, 142, (2017) 2126-2131

[6] Chaoyu Dong, Hongjie Jia, Qianwen Xu, Jianfang Xiao, Yan Xu, Pengfei Tu, Pengfeng Lin, Xiaomeng Li, & Peng Wang 2017b. Time-delay Stability Analysis for Hybrid Energy Storage System with Hierarchical Control in DC Microgrids. IEEE Transactions on Smart Grid, PP, (99)

[7] Chunxia Dou, Dong Yue, Zhanqiang Zhang, & Kai Ma 2017. MAS-Based Distributed Cooperative Control for DC Microgrid Through Switching Topology Communication Network with Time-Varying Delays. IEEE Systems Journal, PP, (99) 1-10

[8] David J.Perreault, Kenji Sato, Robert L.Selders, & John G.Kassakian 1999. Switching-Ripple-Based Current Sharing for Paralleled Power Converters. IEEE Transactions on Circuits and Systems-I: Fundamental Theory and Applications, 46, (10) 1264-1274

[9] David J.Perreault, Robert L.Selders, & John G.Kassakian 1998. Frequency-Based Current-Sharing Techniques for Paralleled Power Converters. IEEE Transactions on Power Electronics, 13, (4) 626-634

[10] Elkawafi, S., Khalil, A ,.Elgaiyar, A. I., & Wang, J. Delay-dependent stability of LFC in Microgrid with varying time delays, In 2016 22nd International Conference on Automation and Computing (ICAC), Colchester, UK: pp. 354-359.

[11] Enrique Rodriguez-Diaz, Mehdi Savaghebi, Juan C.Vasquez, & Josep M.Guerrero An Overview of Low Voltage DC Distribution Systems for Residential Applications, In the 5th IEEE International Conference on Consumer Electronics (IEEE ICCE-Berlin 2015), pp. 1-6.

[12] Jie Chen 1995. On Computing the Maximal Delay Intervals for Stability of Linear Delay Systems. IEEE Transactions on Automatic Control, 40, (6) 1087-1093

[13] Jie Chen, Guoxiang Gu, & Carl N.Nett A New Method for Computing Delay Margins for Stability of Linear Delay Systems, Lake Buena Vista, FL: pp. 433-437.

[14] Jie Chen & Haniph A.Latchman 1995. Frequency Sweeping Tests for Stability Independent of Delay. IEEE Transactions on Automatic Control, 40, (9) 1640-1645

[15] K.Sun, L.Zhang, Y.Xing, & J.M.Guerrero 2011. A Distributed Control Strategy Based on DC Bus Signaling for Modular Photovoltaic Generation Systems With Battery Energy Storage . IEEE Trans.Power Electron, 26, (10) 3032-3045

[16] Keqin Gu, Vladimir L.Kharitonov, & Jie Chen 2003. Stability of Time-Delay Systems Springer.

[17] Khalil, A., Elkawafi, S., Elgaiyar, A .I., & Wang, J. Delay-dependent stability of DC Microgrid with time-varying delay, In 2016 22nd International Conference on Automation and Computing (ICAC), Colchester, UK: pp. 360-365.

[18] Khalil, A. & Wang, J. A New Method for Estimating the Maximum Allowable Delay in Networked Control of bounded nonlinear systems, In The 17th International Conference on Automation and Computing, Huddersfield, UK: pp. 80-85.

[19] Khalil, A. F. & Wang, J. A new stability and time-delay tolerance analysis approach for Networked Control Systems, In 49th IEEE Conference on Decision and Control (CDC), Atlanta, GA, pp. 4753-4758.

[20] Lei Ding, Qing-Long Han, Le Yi Wang, & Eyad Sindi 2018. Distributed Cooperative Optimal Control of DC Microgrids with Communication Delays. IEEE Transactions on Industrial Informatics, 1

[21] Lexuan Meng, Qobad Shafiee, Giancarlo Ferrari Trecate, Houshang Karimi, Deepak Fulwani, Xiaonan Lu, & Josep M.Guerrero 2017. Review on Control of DC Microgrids and Multiple Microgrid Clusters. IEEE Journal of Emerging and Selected Topics in Power Electronics, 5, (3) 928-948

[22] Li Guo, Yibin Feng, Xialin Li, Chengshan Wang, & Yunwei Li Stability Analysis of a DC Microgrid with Master-Slave Control Structure, In 2014 IEEE Energy Conversion Congress and Exposition (ECCE), pp. 5682-56.89

[23] Mohammad B.Shadmand, Robert S.Balog, & Haitham Abu-Rub 2014. Model Predictive Control of PV Sources in a Smart DC Distribution System: Maximum Power Point Tracking and Droop Control. IEEE Transactions on Energy Conversion, 29, (4) 913-921

[24] P.P., Y.Goyal, & V.Agarwal 2017. A Novel Communication Based Average Voltage Regulation Scheme for a Droop Controlled DC Microgrid. IEEE Transactions on Smart Grid, PP, (99) 1

[25] Tomislav Dragicevic, Xiaonan Lu, Juan C.Vasquez, & Josep M.Guerrero 2016. DC Microgrids—Part II: A Review of Power Architectures, Applications, and Standardization Issues. IEEE Transactions on Power Electronics, 31, (5) 3528-3549

[26] Tomislav Dragicevic, Xiaonan Lu, Juan C.Vasquez, & Josep M.Guerrero 2016. DC Microgrids—Part I: A Review of Control Strategies and Stabilization Techniques. IEEE Transactions on Power Electronics, 31, (7) 4876-4891

[27] Xiaonan Lu, Josep M.Guerrero, & Kai Sun Distributed Secondary Control for DC Microgrid Applications with Enhanced Current Sharing Accuracy, In 2013 IEEE International Symposium on Industrial Electronics, Taipei, Taiwan: pp. 1-6.

[28] Xiaonan Lu, Josep M.Guerrero, Kai Sun, & Juan C.Vasquez 2014. An Improved Droop Control Method for DC Microgrids Based on Low Bandwidth Communication With DC Bus Voltage Restoration and Enhanced Current Sharing Accuracy. IEEE Transactions on Power Electronics, 29, (4) 1800-1812

[29] Y.Gu, X.Xiang, W.Li, & X.He 2014. Mode-Adaptive Decentralized Control for Renewable DC Microgrid With Enhanced Reliability and Flexibility . IEEE Trans.Power Electron, 29, (9) 5072-5080

[30] Yuan-Chih Chang, Chia-Ling Kuo, Kun-Han Sun, & Tsung-Chia Li 2013. Development and Operational Control of Two-String Maximum Power Point Trackers in DC Distribution Systems. IEEE Transactions on Power Electronics, 28, (4) 18521861-

[31] Yuwen Nie, Mi Dong, Wenbin Yuan, Jian Yang, Zhangjie Liu, & Hua Han Stabilization methods of DC Microgrid with distributed control considering communication delay, In 2017 IEEE 3rd International Future Energy Electronics Conference and ECCE Asia (IFEEC 2017 - ECCE Asia), pp. 800-805.

[32] Zhengyu Lin, Jin Du, Jiande Wu, & Xiangning He 2015 Novel Communication Method Between Power Converters for DC Micro-grid Applications. 2015 IEEE First International Conference on DC Microgrids (ICDCM), Atlanta, GA, 2015, pp. 92-96.